

# Coupling driven exclusion and diffusion processes on parallel lanes: boundary induced phase transitions and boundary layers

Bappa Saha and Sutapa Mukherji

*Department of Physics, Indian Institute of Technology, Kanpur-208 016*

(Dated: June 21, 2018)

We study a driven many particle system comprising of two identical lanes of finite lengths. On one lane, particles hop diffusively with a bias in a specific direction. On the other lane, particles hop in a specific direction obeying mutual exclusion rule. In addition, the two lanes are connected with each other through exchange of particles with certain rules. The system, at its two ends, is in contact with particle reservoirs which maintain specific particle densities at the two ends. In this paper, we study boundary-induced phase transitions exhibited by this system and predict the phase diagram using the technique of fixed point based boundary layer analysis. An interesting manifestation of the interplay of two density variables associated with two lanes is found in the shock phase in which the particle density profile across the lane with unidirectional hopping shows a jump discontinuity (shock) from a low to a high density region. The density profile on the diffusion-lane never exhibits a shock. However, the shock in the other lane gives rise to a discontinuity in the slope of the diffusion-lane density profile. We show how an approximate solution for the slope can be obtained in the boundary layer analysis framework.

## I. INTRODUCTION

Asymmetric simple exclusion processes (ASEP) are simple non-equilibrium systems of driven interacting particles. These systems have been studied extensively in the past since they show interesting non-equilibrium behavior such as boundary induced phase transitions [1], spontaneous symmetry breaking[2], phase separation [3] etc. Further, ASEPs serve as simple models to understand intracellular transport processes [4–6], traffic flow [7, 8] etc. The simplest and the most extensively studied ASEP involves a one-dimensional lattice on which particles hop in a specific direction. Particles obey the mutual exclusion rule that forbids two particles from occupying the same site. In the case of a finite lattice, the boundaries of the system are attached to reservoirs which maintain specific densities at the boundaries. Unlike equilibrium systems, these one-dimensional systems with short-range interaction exhibit boundary induced bulk phase transitions in which the boundary rates determine the bulk properties of the system. Distinct transport properties and diverse shapes of particle distribution profiles at different bulk phases result from the subtle interplay of the particle current, the inter-particle interaction and the boundaries of the system.

In intracellular transport processes, various kinds of motor proteins hop on the biopolymers to transport different cellular constituents to definite locations inside the cell. In order to have a closer resemblance with these biological transport processes, different kinds of ASEPs have been proposed up to now. The specific ASEP that we consider here consists of two one-dimensional finite lanes (lattices). On one lane, particles have diffusive motion with a bias. We name this lane as the diffusion-lane. On the other lane, to be called as the ASEP-lane, particles hop in a specific direction obeying the mutual exclusion rule. In addition, between the lanes, there are particle exchange processes which lead to a ‘transverse flux’ of

particles. The indirect mutual interaction between the lanes caused by particle exchange leads to a nontrivial coupling between the particle-densities on the two lanes and as a consequence of this, the phase diagram associated with the ASEP-lane is expected to be significantly different from that of a single lane ASEP. The two-lane model we consider here was proposed earlier in order to model intracellular transport processes realistically. The ASEP lane mimics the hopping of the motor particles along the biopolymers. The diffusive lane in this model replaces the environment in which the motor particles diffuse during time intervals when they are not attached to the biopolymers on which they hop [9]. Later, a similar model was proposed in the context of extraction of membrane tubes by motor particles [10].

In the past, the phase diagram for this model has been obtained under zero ‘transverse flux’ condition between the lanes [11]. The boundary conditions maintained by the boundary reservoirs are also assumed to respect this zero ‘transverse flux’ condition. This condition ensures that despite the exchange processes, the average number of particles on a lane is conserved and as a result, the average particle density across the bulk of the lane remains constant (a flat profile). Further, this zero ‘transverse flux’ condition leads to a functional relation between the two density variables and thus the problem reduces to a single lane problem with an effective current density that is different from the hopping current of the usual single lane ASEP [12]. The nature of the bulk profile and the locations of the boundary layers are also predicted through a fixed point based boundary layer analysis [13]. In this article, allowing a nonzero ‘transverse flux’ between the lanes and unconstrained boundary densities, we attempt to obtain general solutions for the steady-state profiles for this coupled two lane problem.

Due to their simplistic nature, much progress has been made on the simplest single-lane ASEP with open boundaries. In addition to exact solutions [12, 14, 15], there ex-

ist other studies based on domain wall dynamics [16, 17], maximum current principle [1], mean-field theory [12] etc which provide significant insights on boundary induced phase transitions in this system. Some of these approaches have been generalized to systems with different inter-particle interactions [18], disordered hopping rates [19], particle adsorption-desorption processes [20, 21] etc. Apart from these, techniques based on boundary-layer analysis have also been developed to study phase transitions in these systems [22, 23]. This analysis shows that the origin of phase transitions and the nature of the phase boundaries can be understood from the shapes of the steady-state density profile and the location of its boundary layer regions under different boundary conditions. Processes with multi-species [24, 25], multi-lanes [11, 13, 26–28] are more complex since, in general, these processes involve two or more density variables. In order to study these complex processes, boundary layer analysis of reference [22], has been further generalized in [25] by developing a fixed point based boundary layer analysis. This work also provides a holographic interpretation of the method which allows predictions about the bulk profile and bulk phase transitions through a fixed point analysis of the boundary layer region. These studies motivate us to obtain a systematic way to find out how, for the present two-lane problem, the boundary layer or the bulk profile changes with the boundary conditions. Using boundary layer analysis, we solve approximately the steady-state differential equation describing the density profile.

From this study, we conclude that while the average density profile of the diffusion-lane remains less sensitive to the boundary densities, the density profile on the ASEP-lane undergoes significant changes as the boundary densities are changed. The present problem has similarities with single lane ASEP with additional particle adsorption-desorption processes (Langmuir Kinetics). However, in our case, the particle exchange happens with a lane which is also dynamically evolving. This is reflected in the phase diagram whose overall structure is different from that of the single lane ASEP, although similar to the single lane ASEP, here also we find three major phases such as low-density, high-density and shock phases. We follow the conventional rule for naming these phases i.e. in the low- and high-density phases, the major part of the density profile has a value less than or greater than 0.5, respectively, and in the shock phase, there is a localized shock (discontinuity) in the bulk part of the profile separating a low- and a high-density region. We show that the diffusion-lane cannot have a shock. However, the shock in the ASEP-lane affects the diffusion-lane's profile by creating a discontinuity in the slope of its profile. The boundary-layer method provides an approximate but a systematic way to study the slope analytically.

The paper is divided into following sections. In section II, we introduce the model and obtain the corresponding mean-field equations. In section III, we discuss the boundary-layer analysis for the model in detail. Results

and the phase diagram are discussed in Section IV. In section V, we present a summary of our work.

## II. DEFINITION OF THE MODEL AND MEAN-FIELD DESCRIPTION

### A. The model

The model comprises of two lanes each having length  $L$  and  $N$  number of sites with lattice spacing  $a$  ( $L = Na$ ). On one of the lanes, referred as the diffusion-lane, particles move with biased diffusion with rates  $D^+$  and  $D^-$  ( $D^+ \neq D^-$ ) towards their right and left, respectively. On the other lane, referred as the ASEP-lane, particles move towards the neighboring site on the right respecting exclusion principle. We assume that a particle hops to the target site with unit probability if the target site is empty. In addition, there are particle exchange processes from one lane to the other. A particle from a diffusion-lane can leave its lane and occupy a site of the ASEP-lane provided the site is empty. We assume that this process takes place at rate  $\omega_a$ . Similarly, a particle from the ASEP-lane can detach itself from its lane and occupy a site on the diffusion-lane at a rate  $\omega_d$ .

Finally, it is assumed that both the lanes are connected at the boundaries to particle reservoirs which maintain specific densities at the two ends of the lanes.

### B. Mean-field equations

We denote the particle-occupancies of the  $i$ -th site of the ASEP- and diffusion-lane by  $\tau_i$  and  $\sigma_i$ , respectively.  $\tau_i = 1, 0$  ( $\sigma_i = 1, 0$ ) imply that the  $i$ th site of the ASEP-lane (diffusion-lane) is occupied or unoccupied, respectively. In terms of these variables, the discrete Master equations describing the particle dynamics have the following forms [11]

$$\frac{d\tau_i}{dt} = -\tau_i(1 - \tau_{i+1}) + \tau_{i-1}(1 - \tau_i) - \tau_i\omega_d + \omega_a\sigma_i(1 - \tau_i) \quad (1)$$

$$\frac{d\sigma_i}{dt} = D^- \sigma_{i+1} - D^+ \sigma_i + D^+ \sigma_{i-1} - D^- \sigma_i + \tau_i\omega_d - \omega_a\sigma_i(1 - \tau_i). \quad (2)$$

A statistical averaging of these master equations along with the assumption that the occupancy variables are uncorrelated i.e.  $\langle \tau_i \tau_{i+1} \rangle = \langle \tau_i \rangle \langle \tau_{i+1} \rangle$  leads to the mean-field equations. Further, we go over to the continuum limit, which implies  $N \rightarrow \infty$ ,  $a \rightarrow 0$  with  $L = Na$  finite. For simplicity, we choose the lattice size to be unity ( $L = 1$ ). In the continuum limit, mean-field equations under steady-state condition ( $\frac{\partial \langle \tau_i \rangle}{\partial t'} = \frac{\partial \langle \sigma_i \rangle}{\partial t'} = 0$ , where  $t'$  is the appropriate rescaled time) are

$$\epsilon \frac{\partial^2 \tau}{\partial x^2} - \frac{\partial \tau}{\partial x} (1 - 2\tau) - \Omega_d \tau + \Omega_a \sigma (1 - \tau) = 0 \quad (3)$$

$$\epsilon D_\sigma \frac{\partial^2 \sigma}{\partial x^2} - v \frac{\partial \sigma}{\partial x} + \Omega_d \tau - \Omega_a \sigma (1 - \tau) = 0, \quad (4)$$

Here  $\Omega_a = \omega_a N$ ,  $\Omega_d = \omega_d N$ ,  $\epsilon = 1/N$ ,  $v = D^+ - D^-$ ,  $D_\sigma = (D^+ + D^-)/2$  and  $\tau(x)$  and  $\sigma(x)$  are the average densities at position  $x$  on the ASEP- and diffusion-lane, respectively. In order to obtain the continuum version from the discrete one, a Taylor-expansion as  $\langle \tau_{i\pm 1} \rangle = \tau(x) \pm \epsilon \frac{d\tau(x)}{dx} + \frac{\epsilon^2}{2} \frac{d^2 \tau}{dx^2}$  and the same for  $\langle \sigma_{i\pm 1} \rangle$  have been done. The second order derivatives in (3) and (4) originate from the second order terms in the Taylor expansion. These second order derivative terms play an important role in the boundary-layer analysis discussed below. In order to obtain the steady-state density profiles, one requires to solve the differential equations with given boundary densities maintained by the boundary reservoirs. We assume that the boundary densities at left end and right end are  $\alpha$  and  $\gamma$  i.e.  $\tau(x=0) = \sigma(x=0) = \alpha$  and  $\tau(x=1) = \sigma(x=1) = \gamma$ .

The total horizontal current in the system is

$$J_{\text{tot}} = J_\tau + J_\sigma = \tau(1 - \tau) + v\sigma, \quad (5)$$

where  $J_\tau = \tau(1 - \tau)$ ,  $J_\sigma = v\sigma$  are the particle currents in the ASEP- and diffusion-lane, respectively. In addition, there is also a ‘transverse particle flux’,  $T = \Omega_a \sigma(1 - \tau) - \Omega_d \tau$ , from one lane to the other arising from the particle exchange processes.

An assumption that the net ‘transverse flux’ is zero ( $T = 0$ ) implies a relation between the two densities  $\sigma = \frac{\Omega_d}{\Omega_a} \frac{\tau}{1 - \tau}$ . Earlier studies [11, 13], based on this assumption, were largely simplified because of this relation. In this work, we assume  $T \neq 0$ . In order to obtain the steady-state density profiles, one has to, therefore, solve two coupled nonlinear equations for two densities under various boundary conditions. In the following, we discuss the boundary-layer analysis of this general system.

### III. BOUNDARY-LAYER ANALYSIS

In boundary-layer analysis, based on the relevance of various terms at different length scales, one usually breaks a differential equation into different parts [29]. The approximate differential equations obtained thereby, are solved and the solutions valid over different length scales are matched asymptotically to obtain a uniform approximate solution of the complete original differential equation over the entire domain of interest. The strategy of focusing on the relevant parts of the differential equation at different length scales often simplifies the problem even if the starting equation has a complicated structure.

#### A. Outer or bulk equation

In the thermodynamic limit,  $N \rightarrow \infty$  ( $\epsilon \rightarrow 0$ ), it appears natural to ignore the second order derivative terms

of equations (3) and (4). The resulting differential equations, known commonly as outer equations, are

$$\frac{d\tau_{\text{out}}}{dx} (1 - 2\tau_{\text{out}}) + (\Omega_d \tau_{\text{out}} - \Omega_a \sigma_{\text{out}} (1 - \tau_{\text{out}})) = 0 \quad (6)$$

$$v \frac{d\sigma_{\text{out}}}{dx} - (\Omega_d \tau_{\text{out}} - \Omega_a \sigma_{\text{out}} (1 - \tau_{\text{out}})) = 0, \quad (7)$$

where, a subscript ‘out’ is introduced to identify the densities as solutions of the outer equations. The solutions of these equations, referred in the following as the outer solutions or bulk solutions, describe the major part of the density profiles. It is straightforward to see that the bulk solutions satisfy the condition  $\frac{dJ_{\text{tot}}}{dx} = 0$  which means  $J_{\text{tot}}$  is constant over the region where bulk solutions for both  $\tau$  and  $\sigma$  together prevail. It must, however, be noticed that a solution of a first order equation as mentioned above can satisfy only one boundary condition.

#### B. Inner or boundary-layer equation

Since the density profile must also satisfy the other boundary condition, the entire density profile cannot be described by the outer solution alone. This implies that the density profile must have another distinctly different part, to be called as inner solution or boundary-layer solution, satisfying either of the following conditions. (a) In case the outer solution satisfies one boundary condition, the inner or the boundary layer solution appears near the other boundary in order to satisfy the boundary condition there. For example, in figure (1), the inner solutions for both  $\tau$  and  $\sigma$  satisfy the boundary condition at  $x = 1$  while their outer solutions satisfy the boundary condition at  $x = 0$ .

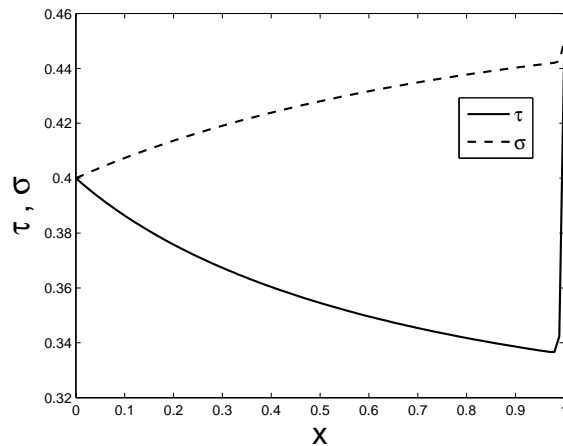


FIG. 1: Density profiles for  $\alpha = 0.4$  and  $\gamma = 0.45$ . Values of other parameters are  $\Omega_d = \Omega_a = 0.2$ ,  $\epsilon = 0.002$ ,  $D_\sigma = 0.6$  and  $v = 0.4$ .

(b) The inner solution may be located somewhere in the interior of the system with two outer solutions appearing on two sides of this solution (shown by the solid

line in figure (2)). Here the inner solution acts like a domain wall separating two outer solutions with high and low density values. Two disjoint outer solution parts satisfy the two boundary conditions. Thus although this solution is referred as inner or boundary-layer solution, it may not necessarily appear near the boundary. In a similar manner, the outer or the bulk solution may start from the boundaries and need not always be confined to the interior of the system.

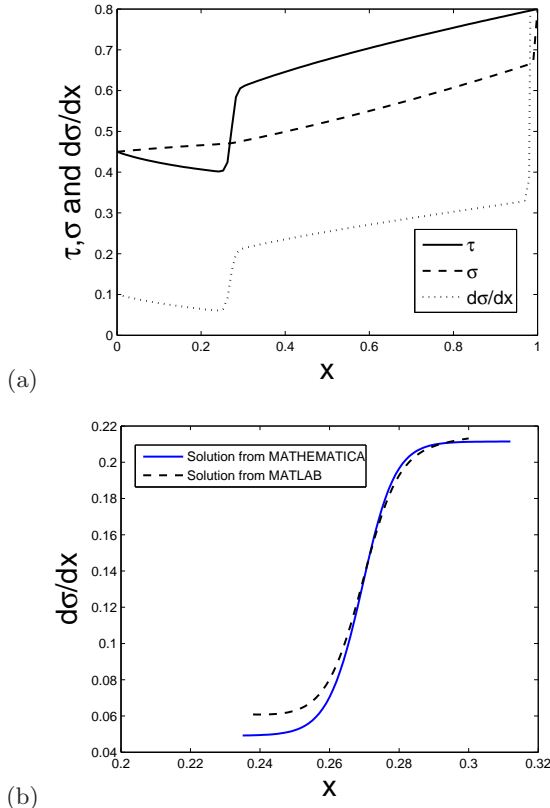


FIG. 2: (a) Density profiles and the slope of  $\sigma$ -profile for  $\alpha = 0.45$  and  $\gamma = 0.8$ . (b) Slope of the  $\sigma$ -profile from analytical and numerical solutions. Other parameter values are same as those in figure (1).

The corresponding differential equation (known as the inner equation) can be found out upon expressing (3) and (4) in terms of a rescaled variable  $\tilde{x} = \frac{x-x_c}{\epsilon}$ , where  $x_c$  represents the location of the boundary layer, and then ignoring terms of  $O(\epsilon)$ . The inner or the boundary layer solution is a rapidly varying solution since it appears over a length scale  $\epsilon$  and becomes sharper as  $\epsilon \rightarrow 0$ . The outer or the bulk solution on the other hand is a much slowly varying solution.

Since the two independent bulk solutions appearing on either side of the inner solution in figure (2) are the solutions of a first order outer equation, each outer solution has one integration constant. These constants are fixed by claiming that each bulk solution satisfies one boundary condition. The boundary layer located at  $x = x_c$ , on

the other hand, merges to the outer solutions smoothly as  $\tilde{x} \rightarrow \pm\infty$ . The constraints on the inner solution are different when the inner solution appears near one boundary. In this case, the inner solution at one end satisfies the boundary condition and on the other end merges to the bulk (see figure (1)). More explicitly, an inner solution near  $x = x_c \approx 0$  or  $x = x_c \approx 1$ , approaches the bulk as  $\tilde{x} \rightarrow \infty$  or  $-\infty$ , respectively. In any case, since the boundary layer has to satisfy more than one condition, it is expected that the inner equation is a higher order equation in comparison with the outer equation. In terms of  $\tilde{x}$  introduced before, we have second order inner equations as shown below.

$$D_\sigma \frac{\partial^2 \sigma_{\text{in}}}{\partial \tilde{x}^2} = v \frac{\partial \sigma_{\text{in}}}{\partial \tilde{x}}, \quad (8)$$

$$\frac{1}{2} \frac{\partial^2 \tau_{\text{in}}}{\partial \tilde{x}^2} = \frac{\partial \{\tau_{\text{in}}(1 - \tau_{\text{in}})\}}{\partial \tilde{x}}. \quad (9)$$

In the following analysis, the density profile will be primarily characterized by the location and the slope of the boundary layer as well as the bulk solutions. These properties depend on whether a particular boundary-layer solution is able to satisfy all the constraints under given boundary conditions.

### C. The boundary layer, the bulk solutions and matching of the two

Bulk solutions can be obtained by solving the nonlinear coupled equations (6) and (7). It appears that it is more convenient to solve the equations numerically with given boundary conditions.

As we shall show below, for our purpose, it is sufficient to have a knowledge about the signs of the slopes of the densities with  $x$ . The slope of the outer solutions can be specified conveniently in  $\tau - \sigma$  plane (see figure 3). It is clear from equations (6) and (7) that, the line  $\sigma_{\text{out}} = \frac{\Omega_d}{\Omega_a} \frac{\tau_{\text{out}}}{(1-\tau_{\text{out}})}$  plays an important role in deciding the slopes.

The inner equations, (8) and (9), are decoupled and can be solved exactly. To obtain the inner solution for the density on the diffusion-lane, we integrate (8) once and find

$$\frac{d\sigma_{\text{in}}}{d\tilde{x}} = \frac{v}{D_\sigma} \sigma_{\text{in}} + \frac{C_\sigma}{D_\sigma}, \quad (10)$$

where  $C_\sigma$  is the integration constant. Since the boundary layer is expected to saturate to the bulk value ( $\frac{d\sigma_{\text{in}}}{d\tilde{x}} = 0$ ) in the appropriate limit, it requires  $C_\sigma = -v\sigma_0$ , where  $\sigma_0$  is the value of the bulk density to which the boundary layer saturates. In terms of  $\sigma_0$ , the solution of (10) is

$$\sigma_{\text{in}} = \frac{D_\sigma}{v} \left[ \exp\left(\frac{v}{D_\sigma}(\tilde{x} + k_0)\right) \right] + \sigma_0, \quad (11)$$

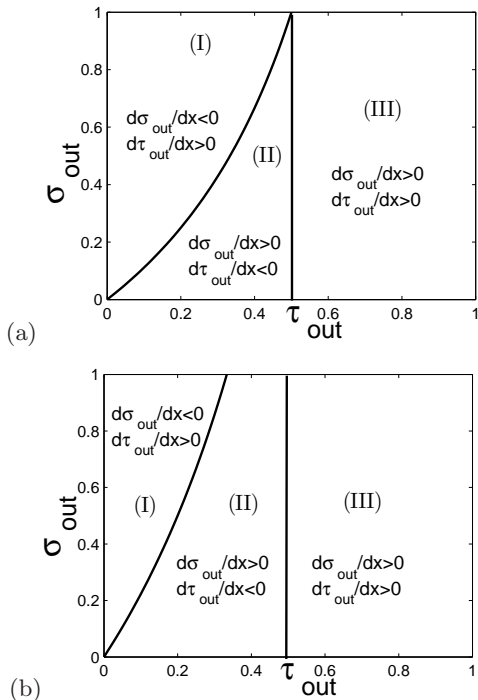


FIG. 3: The signs of the slopes of outer solutions for different values of  $\tau$  and  $\sigma$ . The solid curve corresponds to  $\sigma_{\text{out}} = \frac{\Omega_d}{\Omega_a} \frac{\tau_{\text{out}}}{1-\tau_{\text{out}}}$ . (a) for  $\Omega_d = \Omega_a = 0.2$ ,  $v = 0.4$  and (b) for  $\Omega_d = 2\Omega_a = 0.2$ ,  $v = 0.4$ .

where  $k_0$  is the second integration constant. If the boundary layer appears near  $x = x_c \approx 0$ , the saturation to the bulk density is expected in the  $\tilde{x} \rightarrow \infty$  limit. The exponential solution, diverging as  $\tilde{x} \rightarrow \infty$ , however, can never saturate to the bulk. This restricts the boundary-layer solution for  $\sigma$  to only  $x = 1$  with the slope of the boundary layer at  $x = 1$  being governed by the equation

$$\frac{d\sigma_{\text{in}}}{d\tilde{x}} = (\gamma - \sigma_0) \frac{v}{D_\sigma}. \quad (12)$$

Through this observation, our question about the location of the boundary layers is partly solved. This feature, in addition, is useful for us since we now know that, irrespective of the nature of  $\tau$ -profile and the values of the boundary densities, the outer solution of  $\sigma$  must satisfy the boundary condition at  $x = 0$  and this outer solution must continue until the other boundary where the boundary condition is satisfied by a narrow boundary layer as given in equation (11).

In a similar way, the inner solution for the ASEP-lane can be obtained by integrating (9) once. As done before for the diffusion-lane, here also the integration constant is fixed by demanding saturation of the inner solution to the bulk density  $\tau_0$ . The inner equation thus obtained is

$$\frac{1}{2} \frac{d\tau_{\text{in}}}{d\tilde{x}} = \tau_{\text{in}}(1-\tau_{\text{in}}) + C_\tau = -(\tau_{\text{in}} - \tau_0)(\tau_{\text{in}} - 1 + \tau_0), \quad (13)$$

where  $C_\tau = -\tau_0(1 - \tau_0)$  is the integration constant.

The fixed points of this equation are  $\tau_{\pm}^* = \frac{1 \pm \sqrt{1+4C_\tau}}{2} = (1-\tau_0), \tau_0$  (We have chosen  $\sqrt{1+4C_\tau} = 1-2\tau_0$ ). A linear stability analysis about these fixed points shows that  $\tau_+^*$  is stable (unstable) if  $\tau_0 < 0.5$  ( $\tau_0 > 0.5$ ). Similarly,  $\tau_-^*$  is stable (unstable) if  $\tau_0 > 0.5$  ( $\tau_0 < 0.5$ ). Figure (4) shows

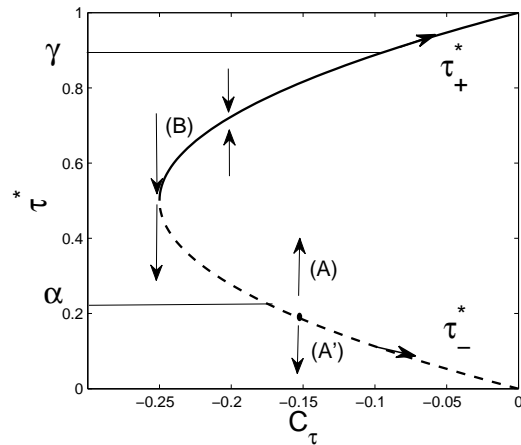


FIG. 4: Fixed points of equation (13) are plotted as functions of  $C_\tau$  for  $\tau_0 < 0.5$ . Solid and dashed curves are referred in the text as upper and lower fixed point branches. Vertical lines with arrows are the flow trajectories. Arrows on the upper and lower fixed point branches indicate that the outer solution is an increasing or decreasing function of  $x$  for  $\tau > 0.5$  and  $\tau < 0.5$ , respectively. Positive and negative slopes of the outer solution correspond to region III and region II of figure (3), respectively.

the two fixed point branches along with the flow behavior indicated through vertical upward or downward arrows.

Equation (9) can be also solved explicitly. The solutions are

$$\begin{aligned} \tau_{\text{in}} &= \frac{1}{2} + \frac{(1-2\tau_0)}{2} \coth[(\tilde{x} + k_1)(1-2\tau_0)] \quad \text{or} \\ \tau_{\text{in}} &= \frac{1}{2} + \frac{(1-2\tau_0)}{2} \tanh[(\tilde{x} + k_1)(1-2\tau_0)]. \end{aligned} \quad (14)$$

From the nature of these solutions in the  $\tilde{x} \rightarrow \pm\infty$  limit, it is clear that while the flow trajectories from the lower to the upper fixed point branch represent the tanh solutions, the trajectories approaching the upper fixed point branch from above or moving further below from the lower fixed point branch represent coth solutions. Although we have explicit analytical solutions for the boundary layers, these are not absolutely required for predicting the qualitative shape of the density profile and the location of the boundary layer under different boundary conditions.

#### IV. PHASE DIAGRAM AND PHASE BOUNDARIES

Here we primarily use the fixed point diagram (figure 4) and the diagram indicating the slopes of the outer so-

lutions (figure 3) to predict shapes of the density profiles under different boundary conditions. In order to do this, the following aspects may be useful. (i) In general, the boundary conditions  $\tau(x=0) = \alpha$  and  $\tau(x=1) = \gamma$  can be marked by two horizontal lines on the fixed point diagram. As shown in figure (4), these lines intersect the fixed point branches at given points. (ii) The major part of the density profile is described by the outer solutions whose decreasing or increasing nature with  $x$  can be predicted with the help of figure (3). The sign of the slope of the outer solution can also be conveniently indicated with arrows on the fixed point curves ( see figure 4). For example, arrows on upper and lower fixed point branches indicate that the density in the outer solution increases or decreases with  $x$ , respectively. The decreasing nature of the outer solution for  $\tau < 0.5$  corresponds to region II in figure (3). It can be argued that all the  $\tau < 0.5$  cases that we have considered in the following correspond to region II of figure (3). (iii) As mentioned earlier, the arrowed vertical lines represent different kinds of boundary-layer solutions obtained earlier. The direction of the arrow in a vertical line of figure (4) indicates where the boundary layer (represented by the vertical line) approaches as  $\tilde{x} \rightarrow \infty$ . As an example, the boundary layer in figure (1) is of tanh type and it is represented by, say, a vertical line (A) in figure (4). It must, however, be noted that the boundary layer of figure (1) is just a part of the vertical line whose saturation to  $\tau_0$  in the  $\tilde{x} \rightarrow -\infty$  is apparent from the density profile shown in the figure but the saturation to  $1-\tau_0$  as  $\tilde{x} \rightarrow \infty$  happens at  $x > 1$  which is much beyond our physical region. In this case, the boundary layer satisfies the boundary condition before saturating to a higher value as  $\tilde{x} \rightarrow \infty$ .

While constructing the density profile for given boundary conditions, one may start from, say,  $x=0$  boundary and construct the density profile until  $x=1$ . Boundary conditions can be satisfied by boundary layers or outer solutions. However, the entire construction of the density profile by combining the boundary layer and the outer solution parts must be consistent with the flow trajectories and the sign of the slope of the outer solution.

The phase diagram is broadly divided into two parts,  $\alpha < 0.5$  and  $\alpha > 0.5$ .

### A. $\alpha < 0.5$

#### 1. Low-density (LD) phase

We begin with small values of  $\alpha$  and  $\gamma$  such that both the horizontal lines corresponding to  $\tau = \alpha$  and  $\gamma$  on the fixed point diagram intersect the lower fixed point branch. Since for the  $\sigma$ -profile, the boundary layer can appear only near  $x=1$ , the boundary condition at  $x=0$  is fulfilled by the outer solution which extends up to the other boundary. For the  $\tau$ -profile, directions of arrows on the vertical lines (see figure 4) indicate that the boundary condition at  $x=0$  cannot be satisfied by a boundary

layer. This is because a boundary layer at  $x=0$  must be represented by a vertical line as (A), satisfying the boundary condition at  $x=0$  and finally meeting the upper fixed point branch. Thus near  $x=0$ , the boundary layer saturates to a bulk solution which always has a value higher than 0.5. It follows from the fixed point diagram that a boundary condition  $\tau(x=1) = \gamma < 0.5$  can never be satisfied by such a bulk solution or by a boundary layer connecting this bulk solution.

Since the possibility of a boundary layer at  $x=0$  is ruled out, the density profile must have an outer solution that satisfies the boundary conditions at  $x=0$  and extends up to  $x=1$  with a negative slope. This amounts to moving along the lower fixed point branch in the direction of the arrow starting from the boundary value  $\alpha$ . We stop at a given density which should be the value of the outer solution at  $x=1$ . The outer solution can then be followed by a boundary layer which finally satisfies the boundary condition at  $x=1$ . The nature of the boundary layer at  $x=1$  is now decided in the following way. If  $\gamma > \alpha$ , the boundary condition at  $x=1$  can be satisfied only through a tanh kind of a boundary layer indicated by the vertical line (A) in figure (4). If  $\alpha > \gamma$ , there can be boundary layers of tanh or coth type depending on the value of  $\tau_{\text{out}}(x=1)$ . For  $\tau_{\text{out}}(x=1) > \gamma$ , a coth type boundary layer of negative slope appears at  $x=1$  (vertical line (A')). A tanh type boundary layer appears at  $x=1$  if  $\tau_{\text{out}}(x=1) < \gamma$  (vertical line similar to (A)). While this tanh type boundary layer saturates to  $\tau_{\text{out}}(x=1)$  as  $\tilde{x} \rightarrow -\infty$ , the saturation to  $1-\tau_{\text{out}}(x=1)$  as  $\tilde{x} \rightarrow \infty$  happens much beyond the physical boundary at  $x=1$ . The dashed line between phases IA and IB in figure (5) indicates the change in the slope of the boundary layer at  $x=1$ . This phase boundary is, therefore, the solution of the equation  $\tau_{\text{out}}(x=1) = \gamma$  where  $\tau_{\text{out}}(x=1)$  is a function of  $\alpha$ . We call this phase as the low-density phase since the value of the bulk density remains within the lower half of the fixed point diagram.

In the low-density phase, as  $\gamma$  is increased keeping  $\alpha$  fixed,  $\tau$ -profile continues to have an outer solution identical to that described above until  $\gamma$  reaches the upper fixed point branch. In all these cases, the boundary condition at  $x=1$  is satisfied by a tanh boundary layer.

#### 2. Shock phase

Keeping  $\alpha$  fixed, if  $\gamma$  is increased beyond the upper fixed point branch, the tanh boundary layer for  $\tau$  can no longer satisfy the boundary condition at  $x=1$  as it saturates to  $1-\tau_{\text{out}}(x=1)$  before satisfying the boundary condition. It is at this point that the boundary layer deconfines from the boundary and enters into the bulk. This gives rise to a jump discontinuity (shock) in the density profile and the system enters into a shock phase. Right on the phase boundary between the low-density and the shock phase, the tanh boundary layer is such

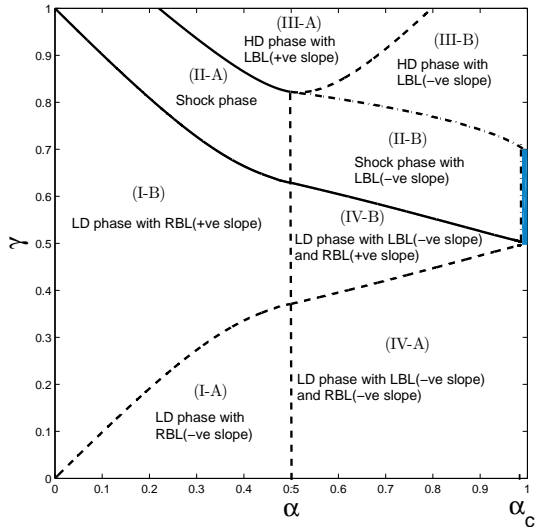


FIG. 5: Phase diagram for  $\epsilon = 0.002$ ,  $D_\sigma = 0.6$ ,  $v = 0.4$ ,  $\Omega_d = \Omega_a = 0.2$ . As the dot-dashed lines are approached from the shock phase, the shock height vanishes continuously. RBL and LBL stand for right boundary layer (boundary layer at  $x = 1$ ) and left boundary layer (boundary layer at  $x = 0$ ), respectively. For this figure as well as figure (9), the vertical dashed line demarcates similar phases with or without LBL. The remaining two dashed curves demarcate two similar phases with change in the slope of a boundary layer only.

that as  $\tilde{x} \rightarrow \infty$ , it saturates exactly at  $\gamma$ . The phase boundary in the  $\gamma - \alpha$  plane is thus determined from the condition  $\gamma = 1 - \tau_{\text{out}}(x = 1)$ , where  $\tau_{\text{out}}(x = 1)$  is a function of  $\alpha$ . In the shock phase, as one increases  $\gamma$  further, the boundary layer moves towards the  $x = 0$  boundary. In this case, as  $\tilde{x} \rightarrow \infty$ , the boundary layer approaches another outer solution part which extends until  $x = 1$  and satisfies the boundary condition there.

The emergence of a shock phase in the phase diagram has similar origin as that observed earlier for a single lane ASEP with Langmuir kinetics [20–22]. However, due to the interplay between the two densities  $\tau$  and  $\sigma$ , we have a much more intriguing situation here. It needs to be noted that while the  $\tau$ -profile here can support a shock (a boundary layer located anywhere in the interior of the lane), a boundary layer for  $\sigma$  is constrained to be only near  $x = 1$ . As seen in figure (2), a jump discontinuity in the  $\tau$ -profile leaves its signature on the  $\sigma$ -profile by producing a discontinuity in the slope of the outer solution of  $\sigma$ . In order to understand this, we study the differential equation for  $k(x) = \frac{d\sigma(x)}{dx}$ . Rewriting (4) as a differential equation for  $k(x)$  and then introducing the scaled variable  $\tilde{x}$ , we have

$$\frac{dk(\tilde{x})}{d\tilde{x}} - \frac{v}{D_\sigma} k(\tilde{x}) + \left[ \frac{\Omega_d}{D_\sigma} \tau_{\text{in}} - \frac{\Omega_a}{D_\sigma} \sigma_c (1 - \tau_{\text{in}}) \right] = 0. \quad (15)$$

We have replaced  $\tau$  by the inner solution  $\tau_{\text{in}}$  since we are interested in probing the region over which the shock

appears in the  $\tau$ -profile. In order to obtain a simpler equation, we have chosen a constant value for  $\sigma$  ( $\sigma = \sigma_c$ ) over the narrow region of the shock. The complementary solution of the differential equation is

$$k(\tilde{x}) = c_1 \exp\left[\frac{v}{D_\sigma} \tilde{x}\right]. \quad (16)$$

This solution diverges exponentially as  $\tilde{x} \rightarrow \infty$  and does not saturate to a finite value as required. This leads us to choose  $c_1 = 0$ . It, therefore, appears that only the particular integral, gives the solution for the slope. Since the shock is a tanh kind solution of the boundary layer, we insert the tanh-solution for  $\tau_{\text{in}}$  in (15) and solve it numerically by supplying values of all necessary parameters such as  $k_1$ ,  $\tau_0$ , that are present in the tanh type solution for  $\tau_{\text{in}}$  and the value of  $x_c$  at which the shock in  $\tau$  is formed. The numerical values of all these parameters are obtained from direct MATLAB solution of the full differential equation under boundary conditions that give rise to a shock in the  $\tau$ -profile. For example, for  $\alpha = 0.45$ ,  $\gamma = 0.8$  and  $\Omega_d = \Omega_a = 0.2$ , the MATLAB solution shows that the shock in  $\tau$  is formed at  $x = x_c = 0.272$  with  $k_1 = -0.065$  and  $\tau_0 = 0.612$ . These numbers are plugged in the tanh solution in (14) which is then used to obtain the particular integral for  $k(\tilde{x})$  numerically using Mathematica.

The particular integral for the slope obtained using Mathematica is compared with the slope obtained from the full numerical solution of the differential equations using MATLAB (see figure (2b)). The mismatch between the solutions away from the center of the shock is possibly due to the approximation of choosing a constant value of  $\sigma$ . From the entire exercise, one may conclude that around the shock, the  $\sigma$ -profile is described by the particular integral of the complete differential equation (4).

### 3. High-density (HD) phase

The high-density phase emerges as the shock reaches the  $x = 0$  boundary with further increase in  $\gamma$ . Hence, right on the phase boundary between the shock and the high-density phase, the tanh type boundary layer saturates to  $\alpha$  at  $x = 0$ . The other end of the tanh solution must saturate to the outer solution which finally extends up to  $x = 1$  boundary and satisfies the boundary condition at  $x = 1$ . Thus right at the phase boundary between the high-density and the shock phase, the outer solution for  $\tau$ -profile, satisfying the boundary condition at  $x = 1$ , has a value  $1 - \alpha$  at  $x = 0$ . As always is the case, the outer solution for  $\sigma$ -profile satisfies the boundary condition at  $x = 0$ . Since, in this phase, the boundary layers for  $\tau$  and  $\sigma$  are located at two opposite boundaries, the strategy to find the phase boundary needs to be altered slightly. We obtain the value of  $\tau_{\text{out}}(x = 1)$  by solving the outer equations for  $\tau$  and  $\sigma$  with boundary conditions  $\tau(x = 0) = 1 - \alpha$  and  $\sigma(x = 0) = \alpha$ . The condition

$\gamma = \tau_{\text{out}}(x = 1)$  finally decides the phase boundary between the shock and the high-density phase.

## B. $\alpha > 0.5$

### 1. Low-density phase

Let us first consider the situation where  $\gamma < 0.5$ . The flow trajectories on the fixed point diagram suggest that there exists only one option through which the density profile is able to satisfy the boundary condition at  $x = 0$  and finally attain a value less than 0.5. This option involves having a boundary layer at  $x = 0$  represented by the vertical line (B) in figure (4). The boundary layer at  $x = 0$  thus saturates to  $\tau = 0.5$  and an outer solution starting from  $\tau = 0.5$  at  $x = 0$  continues with a negative slope until  $x = 1$ . The boundary condition at  $x = 1$  is satisfied by a boundary layer. Depending on the value of the outer solution at  $x = 1$  and the value of  $\gamma$ , the boundary layer has a negative or a positive slope (See figure (6) for a representative  $\tau$ -profile with a boundary layer at  $x = 1$  with positive slope). Similarly

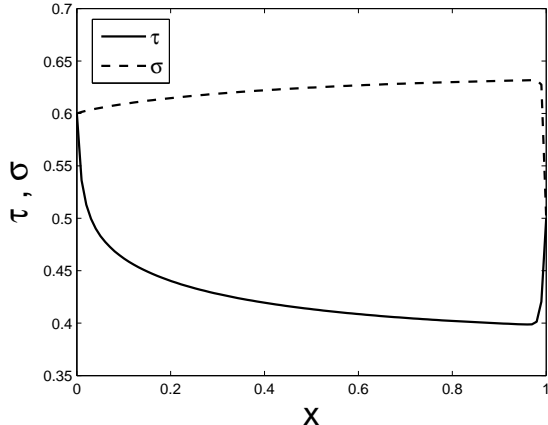


FIG. 6: Representative density profiles in the low-density phase for  $\alpha = 0.6$  and  $\gamma = 0.5$ . The boundary layer at  $x = 1$  has a positive slope. Other parameter values are same as those in figure (1).

to the low-density phase for  $\alpha < 0.5$ , boundary layers in this case also will be represented by vertical lines (A) or (A') of the fixed point diagram. Consequently, the phase boundary between phases IVA and IVB is determined by  $\gamma = \tau_{\text{out}}(x = 1)$ . Since  $\tau_{\text{out}}(x = 1)$  is determined simultaneously by solving the outer equations for  $\tau$  and  $\sigma$  with the conditions  $\sigma(x = 0) = \alpha$  and  $\tau(x = 0) = 0.5$ ,  $\tau_{\text{out}}(x = 1)$  is a function of  $\alpha$ .

### 2. Shock Phase

Keeping  $\alpha$  fixed, as one increases  $\gamma$  further in phase IVB, a shock phase emerges again through the deconfinement of the boundary layer. The shape of the density profile in this phase typically appears as shown in figure (7). The mechanism of shock formation is identical to

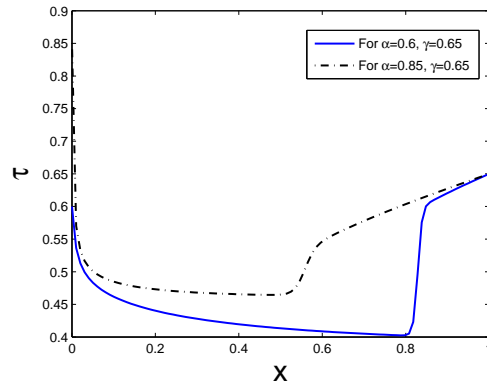


FIG. 7: This figure shows how the  $\tau$ -profile changes in the shock phase as the value of  $\alpha$  is changed keeping  $\gamma$  fixed. Parameter values are same as those in figure (1).

the case of  $\alpha < 0.5$ . Here also, the phase boundary between IVB and the shock phase is determined from the condition  $\gamma = (1 - \tau_{\text{out}}(x = 1))$ . However, in this case,  $\tau_{\text{out}}(x = 1)$  is determined by solving simultaneously the outer equations for  $\tau$  and  $\sigma$  with boundary conditions  $\tau(x = 0) = 0.5$  and  $\sigma(x = 0) = \alpha$ .

For  $\alpha > 0.5$ , the density profiles in the LD and shock phases have negative-slope boundary layers at  $x = 0$  saturating to  $\tau = 0.5$ . Due to this, the outer solution part of the profile always has an effective boundary condition  $\tau(x = 0) = 0.5$  even though the value of  $\alpha$  is changed. The value of  $\tau_{\text{out}}(x = 1)$ , however, is dependent on  $\alpha$  since, in order to find  $\tau_{\text{out}}$ , we have to simultaneously solve (6) and (7) with the boundary conditions  $\sigma_{\text{out}}(x = 0) = \alpha$  and  $\tau_{\text{out}} = 0.5$ . It is because of this dependence that the phase boundaries between phases IVA and IVB and between IVB and the shock phase acquire a slope rather than being horizontal. In order to give a specific example, let us consider phase IVA. In this phase, as  $\alpha$  is increased keeping  $\gamma$  fixed, the outer solution of  $\sigma$ , that satisfies the condition  $\sigma(x = 0) = \alpha$  and continues until  $x = 1$ , in general acquires a larger value. This influences the outer solution for  $\tau$  in such a way that  $\tau_{\text{out}}(x = 1)$  becomes larger as  $\alpha$  increases. Since on the phase boundary between IVA and IVB,  $\gamma$  must be equal to the value of  $\tau_{\text{out}}(x = 1)$ , as  $\alpha$  increases the value of  $\gamma$  also increases leading to a positive slope of the phase boundary. This, in conjunction with the fixed point diagram, implies that the phase boundary between the IVB and the shock phase has a negative slope with  $\alpha$ . The two phase boundaries join when  $\tau_{\text{out}}(x = 1) = 1 - \tau_{\text{out}}(x = 1) = \gamma$ . This corresponds to



$\alpha = \alpha_c = 0.987$  for the parameter values of figure (5). At ( $\alpha = \alpha_c, \gamma = 1/2$ ), the height of the right boundary layer vanishes and a very slowly varying inner solution satisfying the boundary condition at  $x = 0$  and saturating to  $\tau = 0.5$  at  $x = 1$  is present across the whole lane. As a consequence of the disappearance of the right boundary layer, the shock phase terminates at  $\alpha = \alpha_c$  (figure (5)). Therefore, right at the edge of the shock phase, the density profile has a left boundary layer merging to  $\tau = 0.5$ . This is followed by an outer solution which continues until  $x = 1$  and satisfies the boundary condition at  $x = 1$  (see fig (8)). Since  $\gamma > 0.5$  in this figure, the outer solution lies in the upper half of the fixed point diagram. Same trend continues if  $\alpha$  is increased beyond

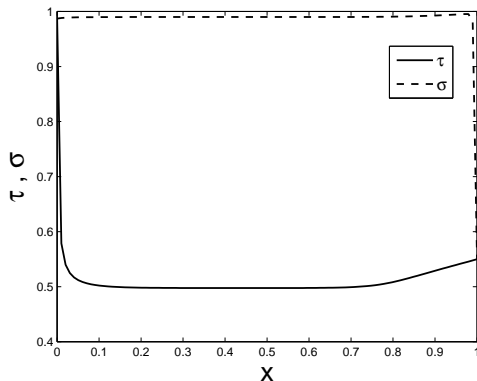


FIG. 8: Density profiles for  $\alpha = 0.987$ ,  $\gamma = 0.55$ . Other parameter values are same as those in figure (1).

$\alpha_c$  (shaded region in figure (5)). From the fixed point diagram and also from the discussion below on the high-density phase, it becomes apparent that for  $\alpha > \alpha_c$ , the shock phase enters into a high-density phase in which the density profile, at  $x = 0$ , has a negative slope boundary layer saturating to an outer solution which has  $\tau > 0.5$  through out.

For  $\Omega_d = 2\Omega_a$ , and parameter values as shown in figure (9),  $\alpha_c > 1$ . The termination of the shock phase is, therefore, not seen in this case.

### 3. High-density phase

In the shock phase, keeping  $\alpha$  fixed at a value sufficiently away from  $\alpha = 0.5$  line, if we increase  $\gamma$ , we expect the shock to be pushed towards the  $x = 0$  boundary. From the continuity point of view, this process should also be accompanied by a reduction of the shock height as the density profile in all these cases, already has a negative slope boundary layer at  $x = 0$  merging to  $\tau = 0.5$  (see figure (10)). The reduction of the shock height is such that right at the phase boundary between the shock and the high-density phase, the shock height disappears. At the phase boundary, the density profile, therefore, has a boundary layer of negative slope at  $x = 0$  followed by

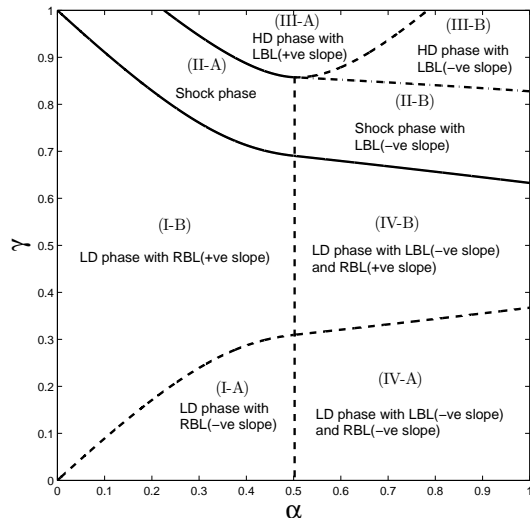


FIG. 9: Phase diagram for  $\epsilon = 0.002$ ,  $D_\sigma = 0.6$ ,  $v = 0.4$ ,  $\Omega_d = 2\Omega_a = 0.2$ . As the dot-dashed phase boundary is approached from the shock phase, the shock height vanishes continuously.

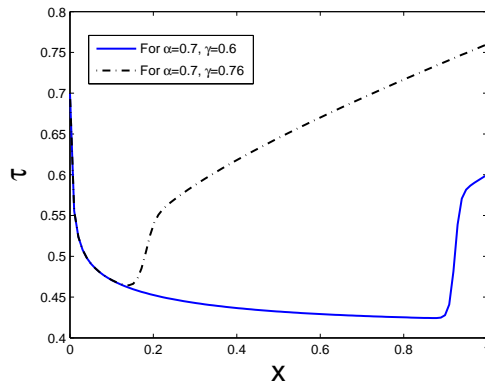


FIG. 10:  $\tau$ -profiles presented here show how the height and the location of the shock change as  $\gamma$  is changed keeping  $\alpha$  fixed. Parameter values are same as those in figure (1).

an outer solution of positive slope satisfying the boundary condition at  $x = 1$ . This outer solution as before lies completely in the upper half of the fixed point diagram. The phase boundary between the shock and the HD phase here is found by the condition  $\tau_{\text{out}}(x = 1) = \gamma$  where  $\tau_{\text{out}}(x = 1)$  is found by solving simultaneously the outer equations for  $\sigma$  and  $\tau$  with boundary conditions  $\tau(x = 0) = 0.5$  and  $\sigma(x = 0) = \alpha$ .

The phase boundary again has an  $\alpha$  dependence. We take the example of this phase boundary to compare our result with single-lane ASEP with Langmuir Kinetics [20]. In the latter case, the outer equation describing the density profile on the lane, has a form [22]

$$\frac{d\tau_{\text{out}}}{dx}(2\tau_{\text{out}} - 1) + \Omega(K(1 - \tau_{\text{out}}) - \tau_{\text{out}}) = 0, \quad (17)$$

where  $K = \Omega_a/\Omega_d$  and  $\Omega = \Omega_d$ . Since, in our case, the outer solution for  $\sigma$  satisfies the boundary condition  $\sigma(x = 0) = \alpha$ , we use the approximation that  $\sigma \approx \alpha$  in (6). With this approximation, the present model is equivalent to a single-lane ASEP with Langmuir kinetics with a varying  $K$ . Although there are significant quantitative differences, two HD-shock phase boundaries, one obtained from the approximate single-lane model and other obtained from our original model have qualitative similarities.

## V. SUMMARY

We consider a driven many particle system consisting of two identical lanes of finite length. Particles move with biased diffusion on one lane termed as the diffusion-lane. On the other lane, referred as the ASEP-lane, particles hop in a specific direction obeying mutual exclusion principle. Two lanes mutually interact through the exchange of particles. These particle exchange processes give rise to a ‘transverse particle flux’ between the lanes. The densities at the boundaries of the two lanes are assumed to be controlled by two reservoirs which maintain specific densities at the boundaries. For simplicity, we assume that the boundary densities at left and right ends are same for both lanes. We denote the boundary densi-

ties as  $\alpha$  and  $\gamma$  for left and right ends, respectively. As the boundary densities are changed, the system exhibits boundary induced bulk phase transitions. Boundary induced transitions in such a two-lane system have been studied earlier using a zero ‘transverse particle flux’ condition [10, 11, 13]. In this paper, we study this system with nonzero ‘transverse particle flux’.

By studying the average density profiles on the two lanes, we obtain the phase diagram in the  $\alpha - \gamma$  space. The phase diagram is based on distinct shapes of density profiles across the ASEP-lane. In different phases, the density profile on the ASEP lane changes significantly due to varying locations of the boundary layers and values of the bulk densities. On the other hand, the density profile on the diffusion-lane does not show significant variation with the boundary densities. The boundary layer in the profile is strictly confined to the right end of the lane. Further, this system provides an opportunity to study how the presence of a discontinuity (shock) in the density profile of the ASEP-lane affects the density profile on the diffusion-lane. This is especially interesting for this particular system since the profile on the diffusion-lane cannot have a jump discontinuity in its bulk. We show that the shock in the ASEP-lane produces a jump discontinuity in the slope of the density profile on the diffusion lane.

- 
- [1] Krug J, 1991 *Phys. Rev. Lett.* **67** 1882.
  - [2] Evans M R, Foster D P, Godrèche C and Mukamel D, 1995 *Phys. Rev. Lett.* **74** 208
  - [3] Janowsky S A and Lebowitz J L, 1992 *Phys. Rev. A* **45** 618.
  - [4] Hirokawa N, 1998 *Science* **279** 519
  - [5] Chou T and Lohse D, 1999 *Phys. Rev. Lett.* **82** 3552
  - [6] Howard J, 2001 *Mechanics of Motor Proteins and the Cytoskeleton* (Sunderland, MA: Sinauer Associates)
  - [7] Mukamel D, 2000 *Soft and Fragile Matter: Nonequilibrium dynamics, Metastability and Flow* (Bristol: IoP Publishing)
  - [8] Helbing D, 2001 *Rev. Mod. Phys.* **73** 1067
  - [9] Klumpp S and Lipowsky R, 2003 *J. Stat. Phys.* **113** 233
  - [10] Tailleur J, Evans M R and Kafri Y, 2009 *Phys. Rev. Lett.* **102** 118109
  - [11] Evans M R, Kafri Y, Sugden K E P and Tailleur J, 2011 *J. Stat. Mech.* P06009
  - [12] Derrida B, Domany E and Mukamel D, 1992 *J. Stat. Phys.* **69** 667
  - [13] Yadav V, Singh R and Mukherji S, 2012 *J. Stat. Mech.* P04004
  - [14] Derrida B, Evans M R, Hakim V and Pasquier V, 1993 *J. Phys. A: Math. Gen.* **26** 1493
  - [15] Schütz G and Domany E, 1993 *J. Stat. Phys.* **72** 277
  - [16] Kolomeisky A B, Schütz G M, Kolomeisky E B and Straley J P, 1998 *J. Phys. A: Math. Gen.* **31** 6911
  - [17] Santen L and Appert C, 2002 *J. Stat. Phys.* **106** 187
  - [18] Hager J S, Krug J, Popkov V and Schütz G M, 2001 *Phys. Rev. E* **63** 056110
  - [19] Harris R J and Stinchcombe R B, 2005 *Phys. Rev. E* **71** 026110
  - [20] Parmeggiani A, Franosch T and Frey E, 2004 *Phys. Rev. E* **70** 046101
  - [21] Evans M R, Juhász R and Santen L, 2003 *Phys. Rev. E* **68** 026117
  - [22] Mukherji S and Bhattacharjee S M, 2005 *J. Phys. A: Math. Gen.* **38** L285
  - [23] Mukherji S, 2007 *Phys. Rev. E* **76** 011127
  - [24] Popkov V, 2007 *J. Stat. Mech.* P07003
  - [25] Mukherji S, 2009 *Phys. Rev. E* **79** 041140
  - [26] Popkov V. and Salerno M, 2004 *Phys. Rev. E* **69** 046103
  - [27] Melbinger A, Reichenbach T, Franosch T and Frey E, 2011 *Phys. Rev. E* **83** 031923
  - [28] Schiffmann C, Appert-Rolland C and Santen L, 2010 *J. Stat. Mech.* P06002
  - [29] Cole J D, 1968 *Perturbation Methods in Applied Mathematics* (Waltham, MA: Blasidal Publishing company)